Available online at www.sciencedirect.com
ScienceDirect
Journal of Nuclear Materials 373 (2008) 259–268
journal of nuclear materials
www.elsevier.com/locate/jnucmat

Synthesis and characterization of mixed An(IV)An(III) oxalates (An(IV) = Th, Np, U or Pu and An(III) = Pu or Am)

B. Arab-Chapelet [a], S. Grandjean [a], G. Nowogrocki [b], F. Abraham [b,*]

[a] Laboratoire de Chimie des Actinides, CEA VALRHO/DRCP/SCPS, Bât. 399, BP 17171, 30207 Bagnols sur Cèze cedex, France
[b] UCCS – Equipe Chimie du Solide, UMR CNRS 8181, ENSCL-USTL, B.P. 90108, 59652 Villeneuve d'Ascq cedex, France

Received 29 January 2007; accepted 7 June 2007

Abstract

The reaction of a solution containing a tetravalent actinide An(IV), a trivalent actinide An(III) and a single-charged cation such as hydrazinium in the presence of oxalic acid in an acidic medium under controlled conditions leads to the precipitation of mixed An(IV)–An(III) oxalate compounds never discussed elsewhere. Two original series were obtained by varying the (An^{IV},An^{III}) pair and the An^{IV}/An^{III} ratio, $(N_2H_5,H_3O)_{2+x}An^{IV}_{2-x}An^{III}_x(C_2O_4)_5\cdot 4H_2O$(**1**) and $(N_2H_5,H_3O)_{1-x}[An^{III}_{1-x}An^{IV}_x(C_2O_4)_2\cdot H_2O]\cdot 4H_2O$(**2**). The crystal structures were identified from powder diffraction patterns by analogy with hydrazinium uranium (IV) lanthanide (III) oxalates whose structures were solved recently by single crystal X-ray diffraction. Complementary investigations by UV–vis and infra-red spectroscopy and thermogravimetric analysis confirm the presence of both tetravalent and trivalent states of actinides in structures (**1**) and (**2**) and the role of single-charged cation and water molecules. The originality of both structures consists in the existence of a mixed crystallographic site for the tetravalent actinide and the trivalent one, the charge balance being ensured by the adjustment of the single-charged ions within the structure. The main difference is that actinides are tenfold coordinated in (**1**) and ninefold coordinated in (**2**). This is the first evidence of a mixed actinide(IV)–actinide(III) site in the same oxalate structure.

1. Introduction

Oxalic precipitation of plutonium(IV) is used at an industrial scale during reprocessing of nuclear fuel by the PUREX process to convert this energetically valuable actinide into oxide form suitable for future use, e.g. as raw material for MOX production. Oxalic acid is also a very common reagent to recover actinides from liquid waste by using precipitation methods because of the very low solubility of An(IV) or An(III) oxalate compounds in acidic solutions. The chemical properties of actinide oxalates have often been investigated but, surprisingly, only few detailed structural determinations are dedicated to such compounds [1]. Previous studies have been devoted to crystallographic structures of simple oxalates of actinide(IV) $An^{IV}(C_2O_4)_2\cdot 6H_2O$ [2,3] and actinide(III) $An^{III}_2(C_2O_4)_3\cdot 10H_2O$ [3] (isomorphic with $Ln_2(C_2O_4)_3\cdot 10H_2O$; Ln = La, Ce, Pr, Nd [4–6]) and of double M^+–An(IV) ($M = K^+$, H^+, An = Th [7], U [8], Np [9]) oxalates. However, mixed An(IV)–An(III) oxalate structures have never been described to date. Recently we published the crystal structure of new mixed M^+–U(IV)–Ln(III) [10–12] oxalate compounds ($M^+ = Na^+$, NH_4^+, $N_2H_5^+$, Ln = Ce, Nd, Sm, Gd) synthesized using a crystal growth method based on slow diffusion of metallic cations through silica gel impregnated with oxalic acid. Single crystal data acquisition led to elucidate new original mixed structures that belong to three series called triclinic, hexagonal and tetragonal. These three families of mixed U(IV)–Ln(III) oxalates are characterized by an unexpected mixed U(IV)–Ln(III) crystallographic site, where U(IV) and Ln(III) are 10-fold coordinated in the hexagonal structure and 9-fold coordinated in the triclinic and tetragonal ones. Monovalent cations equilibrate the charge in these structures depending on the Ln(III)/(U(IV)+Ln(III)) mole

* Corresponding author. Fax: +33 3 20 43 68 14.
E-mail address: francis.abraham@ensc-lille.fr (F. Abraham).

0022-3115/$ - see front matter © 2007 Elsevier B.V. All rights reserved.
doi:10.1016/j.jnucmat.2007.06.004

ratio. The hexagonal and triclinic compounds adopt a honeycomb type structure based on a three-dimensional network of metallic and oxalate ions, while the tetragonal structure is built from a two-dimensional arrangement of squared metal-oxalate cycles.

5f-Actinides are known to exhibit structural behavior similar to that of 4f-lanthanides in many cases. The most obvious analogy is the similar cation size of An^{3+} and Ln^{3+} at a given coordination number [13]: Ce^{3+} and Nd^{3+}correspond to Pu^{3+} and Am^{3+}, respectively. Considering this analogy between An^{3+} and Ln^{3+} in coordination chemistry, structural data recently published about U(IV)–Ln(III) oxalates can be used to identify An(IV)–An(III) co-precipitated compounds.

The silica gel method is a convenient means of promoting crystal growth of oxalate compounds [14,15] but it exhibits major drawbacks: (i) the chemical composition of the resulting crystals cannot be controlled; (ii) only few crystals are synthesized, so full characterization of the resulting compounds using various and often destructive techniques is not possible and (iii) this method is complex to implement in confined environments such as glove-boxes: alpha self-irradiation may induce damage to the crystals during their slow growth; isolation and conservation of sub-millimeter single crystals from the silica gel are moreover a particularly uneasy task.

The present work deals with a thorough investigation of the mixed U(IV)–Ln(III) oxalates synthesized by co-precipitation methods and aims at (i) specifying the solid solution domains; (ii) investigating the transfer of metallic cations initially in solution to the co-precipitated solid, with particular attention to their redox behavior and (iii) clarifying the role of monovalent cations taking part in the charge compensation in the structure. Finally, these co-precipitation experiments were extended to An(IV)–An(III) mixtures (An(IV) = Th, U, Np or Pu and An(III) = Pu or Am) in order to identify and structurally characterize co-precipitated An(IV)–An(III) oxalates.

2. Experimental section

2.1. Reagents

Actinide(IV) and actinide(III) solutions were prepared using specific procedures, either from purified mono-metallic solutions or by dissolving mono-metallic oxides or hydroxides. Hydrazinium nitrate ($N_2H_5^+$, NO_3^-) was used as an anti-nitrous agent to stabilize the lowest oxidation states (typically (IV) for U and Np, and (III) for Pu) and as source of monocharged cations. The concentration, purity and oxidation state were essentially determined by UV–vis spectroscopy. Lanthanide nitrate salts (Aldrich, 99.9% Reagent Grade $Ln(NO_3)_3 \cdot 6H_2O$) were used when appropriate to prepare Ln(III) solutions to simulate An(III) solutions in pseudo-active experiments, considering the similarities between Ln(III) and An(III) ions [13].

2.2. Oxalate co-precipitation experiments

The oxalate co-precipitates were prepared by mixing a solution of An(IV) and An(III) or Ln(III) (An(IV) = Th, U, Np, Pu; An(III) = Pu, Am; and Ln(III) = Nd, Sm) and a concentrated $H_2C_2O_4$ solution (with a slight excess of oxalic acid) in a nitric medium [16]. The selected lanthanides for this work were Nd(III) and Sm(III) which both exhibit UV–vis peaks in the 350–900 nm domain.

The resulting crystallized powders, whose color depends on the elements involved, were filtered off and dried at room temperature. A series of lanthanide–uranium co-precipitates were prepared with Ln/Ln + U mole ratios equal to 0%, 10%, 20%, 30%, 40%, 50%, 60% and 70% (Ln = Nd, Sm). Above 70%, the co-precipitated powder is a polyphase system based on the well-known lanthanide oxalate $Ln_2(C_2O_4)_3 \cdot 10H_2O$ [4–6].

For An(IV)–An(III) mixtures, two mole ratios: (10% and 50%) were studied to investigate the influence of the actinide(IV) and actinide(III) nature and the An(III)/(An(IV) + An(III)) mole ratio on the co-precipitate structure.

2.3. XRD acquisition

X-ray powder diffraction data for all mixed oxalates were obtained with an INEL CPS 120 diffractometer (curved position-sensitive detector) using Cu Kα1 radiation isolated by a germanium monochromator. Silicon was added to all samples as an internal standard to calibrate the angular positions of the observed XRD lines. Actinide oxalates were mixed with an epoxy resin to prevent contamination spreading and their diffraction patterns were compared with the recently built M^+–U(IV)–Ln(III) oxalate structures database [10–12] to detect isomorphic similitude. The lattice parameters of the mixed oxalates were refined by pattern matching using the Fullprof software [17].

2.4. UV–vis spectroscopic analysis

Actinide and lanthanide concentrations in solution were determined by UV–vis spectroscopy using a CINTRA 10e GBC UV spectrophotometer between 350 and 900 nm. Actinide oxidation states in the co-precipitates were investigated in a glove-box using a HITACHI U-3000 spectrophotometer equipped with an integration sphere for reflection measurements.

Hydrazinium cations were quantified by colorimetric analysis: in a 1 M nitric medium, hydrazinium cation reacts with dimethylamino-4-benzaldehyde to form a yellow complex that presents a peak around 455 nm.

2.5. Infrared spectroscopic analyses

Infrared spectra of all samples were recorded with the NICOLET MAGNA IR 550 series II between 400 and 4000 cm^{-1}.

2.6. Thermogravimetric analysis

Thermogravimetric analysis (TGA) was carried out with a NETZSCH STA 409C thermal analysis system with an alumina crucible up to 950 °C, under argon flow and with a heating rate of 10 °C min^{-1} to determine the water content of the freshly synthesized powders.

3. Results and discussion

The first polymetallic systems described below are mixed uranium(IV)–lanthanide(III) oxalates (Ln = Nd, Sm; in these experiments lanthanide(III) simulated actinide(III)), the second ones concern polyactinide An(IV)–An(III) oxalates (An(IV) = Th, U, Np and Pu; An(III) = Pu, Am).

3.1. Uranium(IV)–lanthanide(III) systems

3.1.1. Transfer of the metallic cations to the co-precipitated solid

Using the oxalate ligand, which is known to form very insoluble complexes with An(IV), An(III) and Ln(III) in acidic media, uranium(IV) and lanthanides(III) co-precipitated quantitatively and without modification of either the U(IV)/Ln(III) mole ratio or the oxidation state of U (Figs. 1 and 2). Co-precipitation yields exceeded 99% using the experimental method described above.

3.1.2. Solid solution domains of existence

Previous work on mixed U(IV)–Ln(III) oxalate structures [10–12] indicated that two solid solutions with the generic formulas $M_{2+x}U^{IV}_{2-x}Ln^{III}_{x}(C_2O_4)_5 \cdot nH_2O$ (hexagonal series) and $M_{1-y}U^{IV}_{y}Ln^{III}_{1-y}(C_2O_4)_2 \cdot nH_2O$ (triclinic and quadratic series) (M = monocharged cation) can be expected. The determination of the solid solution domains for the U(IV)–Ln(III) systems requires a thorough investigation of the co-precipitate structure versus the Ln/(U+Ln) mole ratio. Fig. 3 shows the XRD patterns of U(IV)–Ln(III) co-precipitates which were identified by comparison with the theoretical XRD patterns of the recently built M^{+}–U(IV)–Ln(III) oxalate database [10–12] to detect isomorphic similarities.

For neodymium substitution rates of 0–50%, the precipitate is a single-phase oxalate (solid solution) isomorphic to the ammonium uranium (IV) oxalate $(NH_4)_2U_2(C_2O_4)_5 \cdot 0.7\,H_2O$, previously described [10] and which adopts a hexagonal structure (Fig. 3(a)). This single-phase oxalate is characterized by a three-dimensional arrangement of U-centered polyhedra linked through bis-bidentate oxalate groups. The U(IV) atom is 10-fold coordinated by

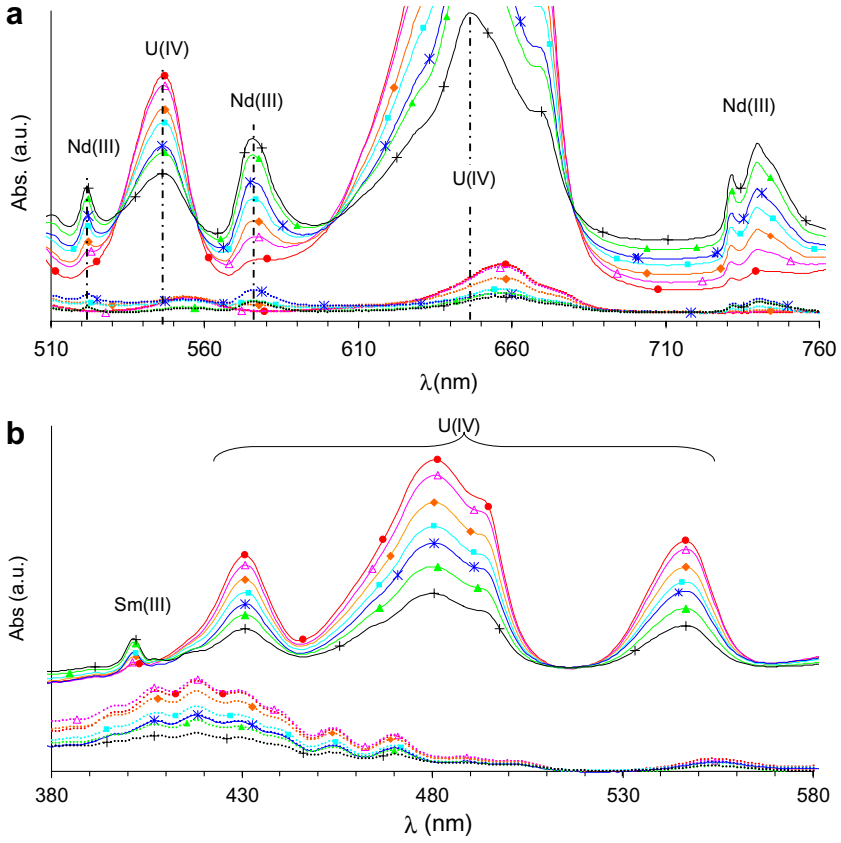

Fig. 1. UV–vis spectra of solution obtained during U(IV)–Ln(III) oxalate precipitation tests: (a) Ln = Nd; (b) Ln = Sm; ● $U_{90}Ln_{10}$; ● $U_{80}Ln_{20}$; ◆ $U_{70}Ln_{30}$; ■ $U_{60}Ln_{40}$; × $U_{50}Ln_{50}$; ● $U_{40}Ln_{60}$; + $U_{30}Ln_{70}$. Solid lines: nitric solution containing U(IV)–Ln(III) mixture *with a dilution factor for spectrum acquisition equal to 1:20*; broken lines: nitric supernatant after oxalate precipitation of metallic cations *without any dilution for spectrum acquisition.*

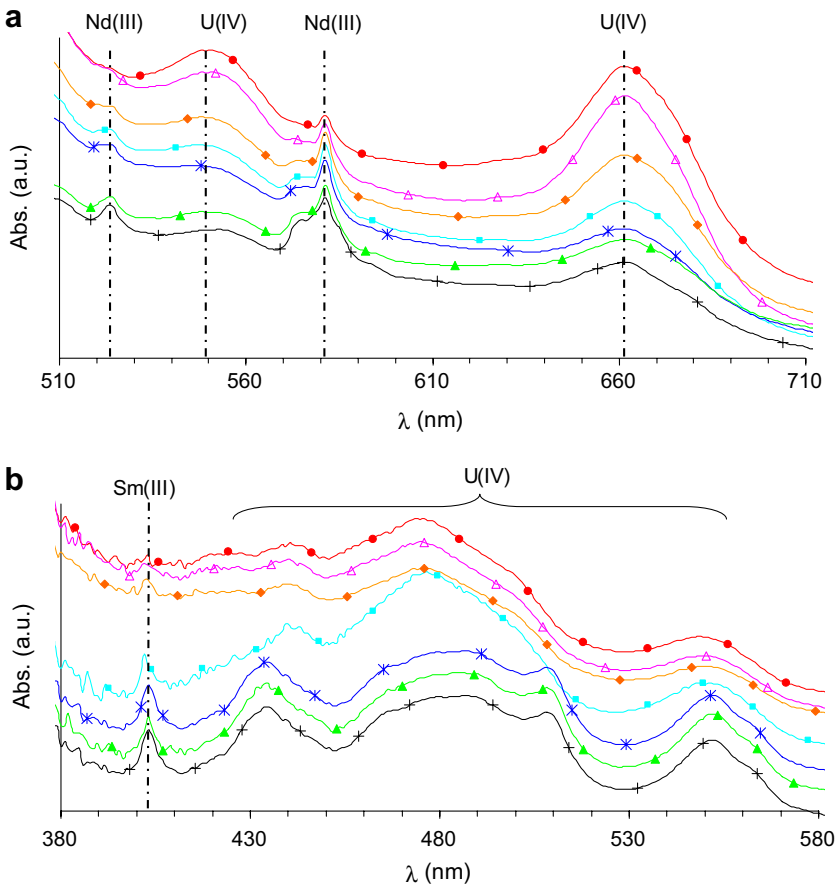

Fig. 2. UV–vis spectra of solids obtained during U(IV)–Ln(III) oxalate precipitation tests showing the invariability of oxidation state during experiments: (a) Ln = Nd; (b) Ln = Sm; ● $U_{90}Ln_{10}$; ● $U_{80}Ln_{20}$; ◆ $U_{70}Ln_{30}$; ■ $U_{60}Ln_{40}$; × $U_{50}Ln_{50}$; ● $U_{40}Ln_{60}$; + $U_{30}Ln_{70}$.

oxygen atoms from five bidentate oxalate groups, but astonishingly U(IV) can be partially substituted by Nd(III) in the same crystallographic site, the charge deficit being compensated by additional monovalent ions. This partial substitution $U(IV) \rightarrow Nd(III) + M^{+}$ does not modify the crystallographic structure of the precipitates. It can occur because the ionic radii of U(IV) and Nd(III) are close, 1.05 and 1.163 Å, respectively (coordination number = IX [18]) and because both ions can exhibit the same type of coordination sphere, for instance, 10 oxygen atoms from five bidentate oxalate ligands.

Beyond 50% substitution, precipitates are composed of a mixture of hexagonal mixed oxalate and neodymium(III) oxalate $Nd_2^{III}(C_2O_4)_3 \cdot 10H_2O$. The linear variation of the unit cell parameters with the Nd/(U + Nd) mole ratio confirms the existence of a hexagonal solid solution with the general formula $M_{2+x}U^{IV}_{2-x}Ln^{III}_x(C_2O_4)_5 \cdot nH_2O$ which is stable within a large composition range ($0 \leqslant Nd/(U + Nd) \leqslant 0.5$, Fig. 4) and also magnificently illustrates the presence within the structure of a mixed U(IV)–Nd(III) crystallographic site.

Concerning the U(IV)–Sm(III) system (Fig. 3(b)), the identification of the XRD patterns of precipitated oxalates thanks to the structural data base is more complex: from 0% to 10% substitution the precipitate consists in a mixture of uranium(IV) oxalate $U(C_2O_4)_2 \cdot 6H_2O$ and U(IV)–Sm(III) hexagonal mixed oxalate; for $0.1 < Sm/(U + Sm) \leqslant 0.3$, there is a hexagonal single-phase compound; for $0.3 < Sm/(U + Sm) \leqslant 0.5$, the resulting powders correspond to a mixture of hexagonal and tetragonal forms. The tetragonal mixed oxalate is built from a bi-dimensional arrangement of metal-oxalate squared cycles. In this structure, U(IV) and Sm(III) occupy the same crystallographic site and this mixed site is 9-fold coordinated by oxygen atoms from four bidentate oxalate ligands and one water molecule. For $0.5 < Sm/(U + Sm) \leqslant 0.7$, the precipitates are tetragonal single-phase oxalates; finally, beyond 0.7, there is a mixture of samarium(III) oxalate and U(IV)–Sm(III) tetragonal mixed oxalate.

The comparison of these structural results with those obtained previously for the U(IV)–Nd(III) system, highlights the evolution of the solid solution domains and types along the lanthanide series. This evolution is not only related to the ionic radii of the Ln(III) ion, the stability range of the U(IV)–Nd(III) hexagonal solid solution is broader than that of the corresponding Sm-analog whereas the ionic radii of U(IV) and Sm(III) are more similar than are U(IV) and Nd(III). In fact the substitution is also accompanied by a variation of the compensating monovalent ion, moreover for 4f and 5f-elements the model of rigid

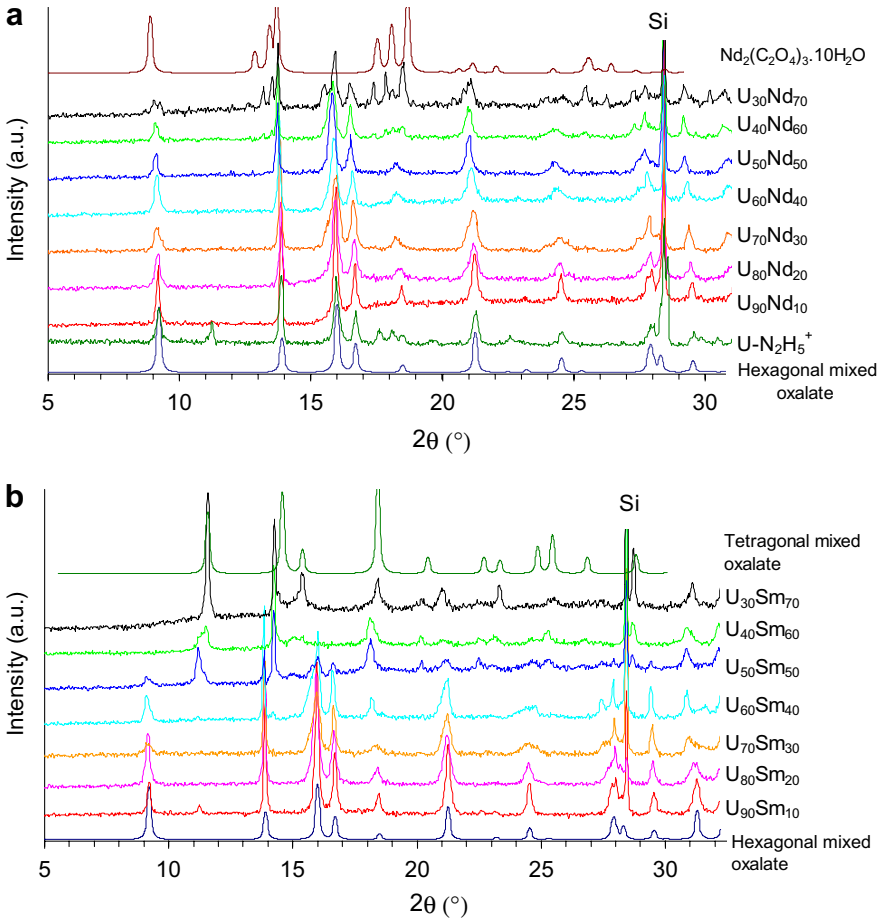

Fig. 3. XRD patterns of U(IV)–Ln(III) oxalate precipitates: (a) Ln = Nd; (b) Ln = Sm.

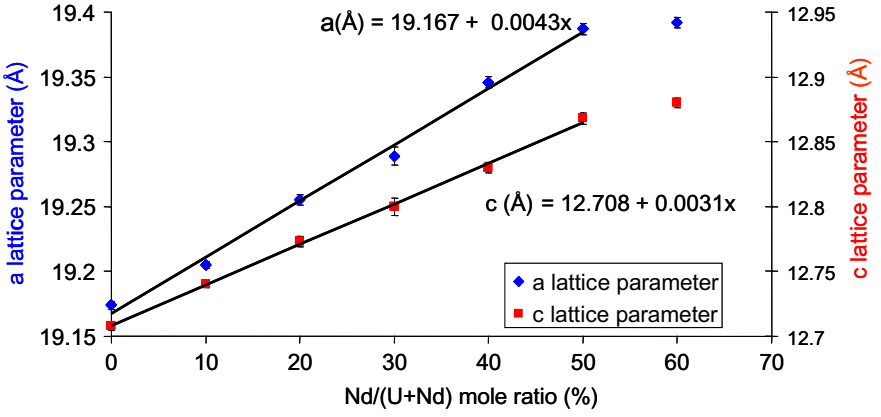

Fig. 4. Determination of Vegard's law for U(IV)–Nd(III) hexagonal solid solution confirming the existence of a large solid solution domain of existence.

spheres is not always satisfactory. Finally for the Sm substitution a tetragonal solid solution is formed. Additional works are necessary to determine the factors which lead to a hexagonal, tetragonal or triclinic phase.

The refinement of the unit cell parameters of the U(IV)–Sm(III) mixed oxalates was more complex because few Sm/(U + Sm) mole ratios produced a single-phase precipitate. However, for single-phases corresponding to Sm/(U + Sm) = 0.2, 0.3 and 0.6, the lattice parameters were refined by pattern matching (Table 1). The decrease in the unit cell parameters of the hexagonal U(IV)–Ln(III) mixed oxalate (Ln = Nd or Sm) from Nd(III)-substituted to Sm(III)-substituted compounds is in agreement with the decrease in the ionic radii along the lanthanide series ($r_{Nd(III)} = 1.163$ Å and $r_{Sm(III)} = 1.132$ Å in ninefold coordination [18]).

Table 1
Lattice parameters of mixed U(IV)–Sm(III) oxalates

$^{Sm}/_{(U+Sm)}$	Structure	a (Å)	c (Å)
0	Hexagonal	19.174(3)	12.707(3)
0.2	Hexagonal	19.217(6)	12.747(5)
0.3	Hexagonal	19.245(6)	12.761(5)
0.6	Tetragonal	8.798(3)	7.874(4)

3.1.3. Identification of monovalent cations

The infrared spectra of U(IV)–Ln(III) precipitates (shown in Fig. 5) are characteristic of oxalate compounds. The infrared bands located at 1650, 1485, 1360, 1320 and 805 cm^{-1} are characteristic to a tetradentate oxalate ligand [19,20]. However, the comparison of these IR spectra with those of lanthanide oxalate $Ln_2^{III}(C_2O_4)_3 \cdot 10H_2O$ and uranium oxalate $U^{IV}(C_2O_4)_2 \cdot 6H_2O$ indicates the presence of two additional bands located at 960 and 930 cm^{-1} which could be assigned to the N–N stretching vibrations of the hydrazinium cation $N_2H_5^+$ [20,21]. The large absorption band between 3000 and 3600 cm^{-1} has been attributed to the ν_{O-H} of water molecule.

The charge compensation in the structure is partially ensured by hydrazinium cations $N_2H_5^+$ located inside the cavities of the crystal network.

Chemical composition analysis (spectrophotometric titration of $N_2H_5^+$ cations) together with TGA to determine the water content for each composition yielded the formulas $(N_2H_5)(H_3O)_{1+x}U^{IV}_{2-x}Ln^{III}_x(C_2O_4)_5 \cdot 4H_2O$ for the hexagonal mixed U(IV)–Ln(III) oxalates and $(N_2H_5, H_3O)_{1-y}U^{IV}_yLn^{III}_{1-y}(C_2O_4)_2 \cdot 4H_2O$ for the tetragonal one. For the hexagonal mixed oxalate compounds, considering the substitution scheme U(IV) → Ln(III) + M^+, the charge balance is ensured by H_3O^+ cations starting from the $(H_3O^+)(N_2H_5^+)U_2(C_2O_4)_5 \cdot 4H_2O$ oxalate compound. For the tetragonal system further investigations are needed to clarify the role of H_3O^+ and $N_2H_5^+$ in the charge balance.

3.2. Actinide(IV)–actinide(III) systems

3.2.1. Transfer of metallic cations to the co-precipitated solid

Investigations by UV–vis spectroscopy confirmed the simultaneous precipitation of all the An(IV) and An(III) involved (An(IV) = Th, U, Np or Pu and An(III) = Pu or Am) without modifying either the An(IV)/(An(III) + An(IV)) mole ratio or the oxidation state (Figs. 6 and 7). The UV–vis spectra of the different precipitated solids confirm the stabilization of a mixture of actinide (III) and (IV)

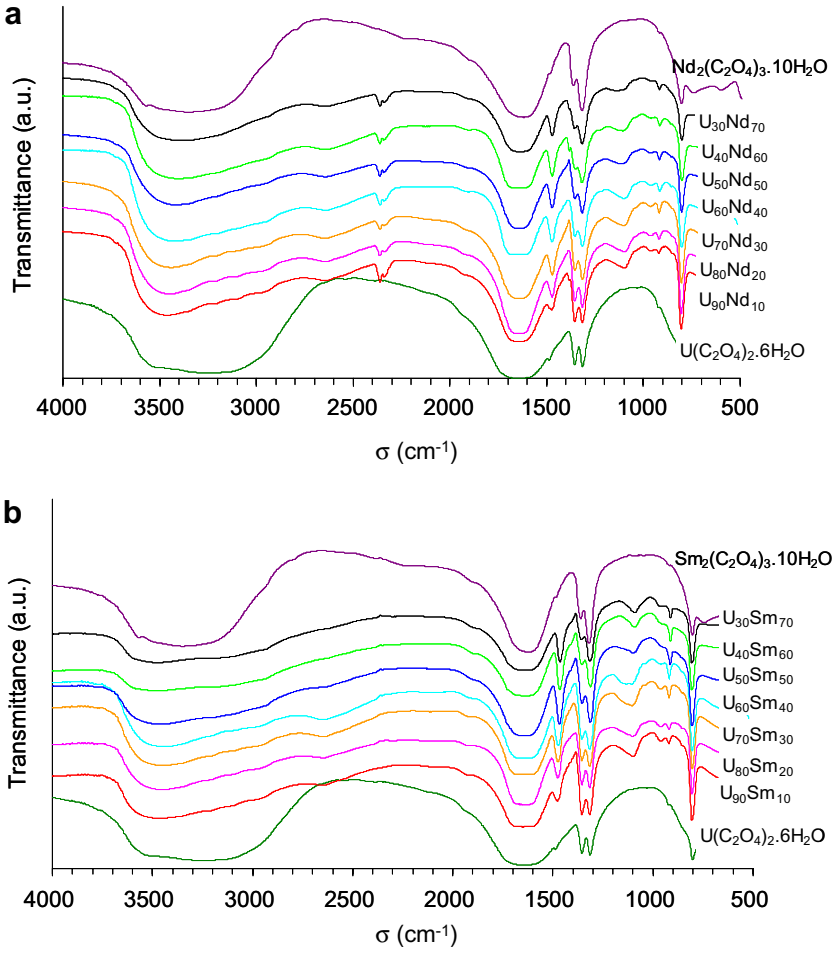

Fig. 5. Infrared spectra of U(IV)–Ln(III) oxalate precipitates: (a) Ln = Nd; (b) Ln = Sm.

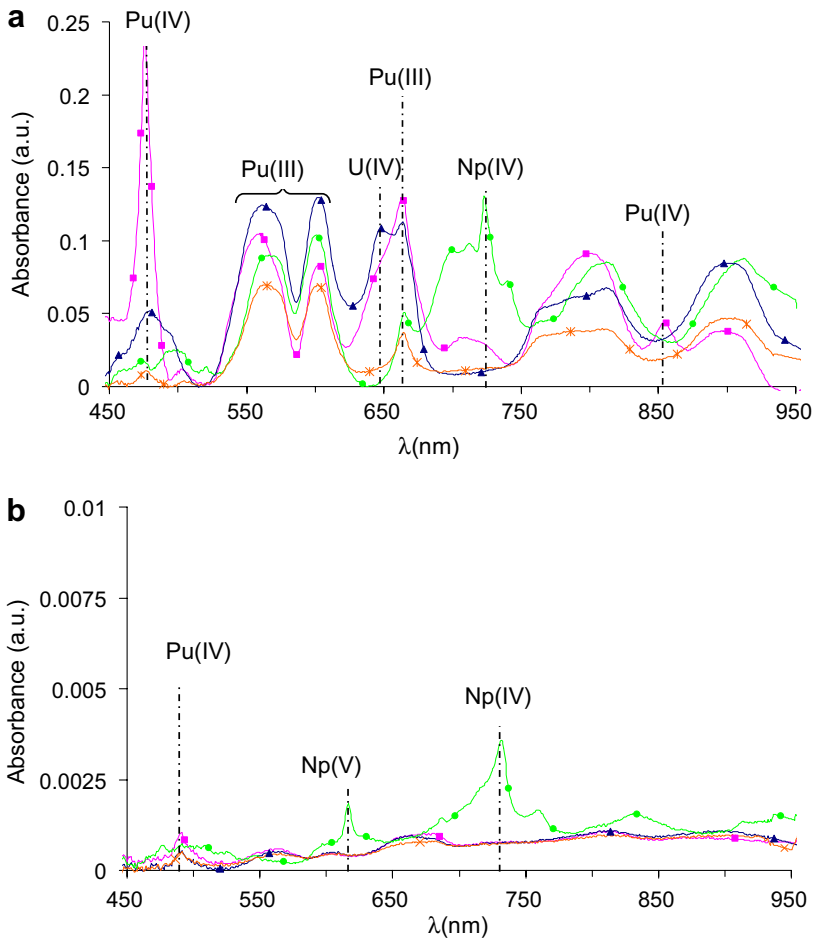

Fig. 6. UV–vis spectra of solutions obtained during An(IV)–Pu(III) oxalate precipitation experiments: (a) nitric solution containing An(IV)–Pu(III) mixture *with a dilution factor for spectrum acquisition equal to 1:20*; (b) nitric supernatant after oxalate precipitation of metallic cations *without any dilution for spectrum acquisition*: ● $Np(IV)_{50}Pu(III)_{50}$; ■ $Pu(IV)_{50}Pu(III)_{50}$; ● $U(IV)_{50}Pu(III)_{50}$; × $Th(IV)_{50}Pu(III)_{50}$.

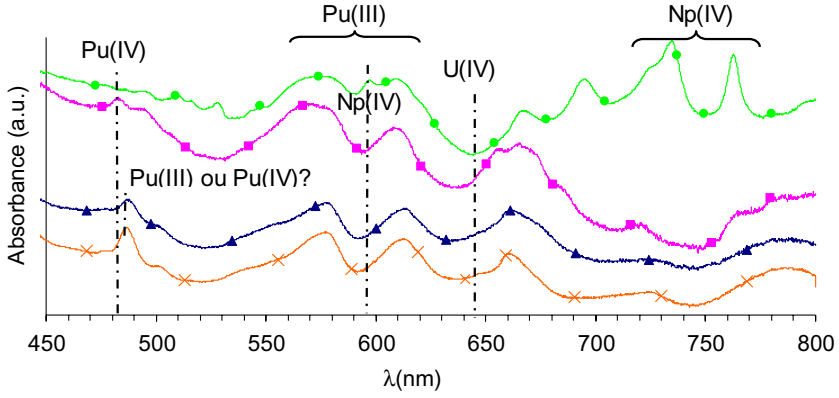

Fig. 7. UV–vis spectra of solids obtained during An(IV)–Pu(III) oxalate precipitation tests showing the invariability of oxidation state during experiments: ● $Np(IV)_{50}Pu(III)_{50}$; ■ $Pu(IV)_{50}Pu(III)_{50}$; ● $U(IV)_{50}Pu(III)_{50}$; × $Th(IV)_{50}Pu(III)_{50}$.

within the same compound. This result is undoubtedly original and more interesting for the Pu(IV)–Pu(III) mixed oxalate in which the two oxidation states of plutonium are stabilized within the same solid phase.

Except for the Np(IV)–Pu(III) experiment, the actinide concentrations in the nitric supernatant after oxalic co-precipitation are very weak (10–30 mg/L). Under controlled conditions, these concentrations are comparable to or even

lower than the values published for $An^{IV}(C_2O_4)_2 \cdot 6H_2O$ [22] and $An_2^{III}(C_2O_4)_3 \cdot 10H_2O$ oxalates. Thus, for Th(IV)–Pu(III), U(IV)–Pu(III), Pu(IV)–Pu(III) (Fig. 6) and U(IV)–Am(III) pairs, the precipitation yields are higher than 99%.

Concerning the Np(IV)–Pu(III) system, even if the co-precipitation yield remains very high (≈92%), the neptunium(IV) concentration (90–100 mg/L) in the nitric supernatant is significant and curiously higher than the solubility of $Np^{IV}(C_2O_4)_2 \cdot 6H_2O$ oxalate [23]. In fact, this result can be explained by the presence of Np(V) (≈5%) in the Np(IV) solution. Np(V) is fully measured in the supernatant, where it reacts slowly with Pu(III) traces according to the redox reaction: $Pu^{3+} + NpO_2^+ + 4H^+ \rightarrow Pu^{4+} + Np^{4+} + 2H_2O$. The Pu(IV) produced by this reaction is subsequently reduced to Pu(III) by hydrazinium nitrate contained in the medium, leading to the reduction of the majority of the Np(V) initially present.

3.2.2. Solid solution domains

The new mixed An(IV)–An(III) (An(IV) = Th, U, Np or Pu and An(III) = Pu or Am) single-phase co-precipitates obtained by oxalic conversion were characterized from powder diffraction patterns by analogy with uranium(IV)–lanthanide(III) oxalates that structures were recently solved from single crystal X-ray diffraction data [10–12]. By varying the (An^{IV}, An^{III}) pair and depending on the An^{IV}/An^{III} mole ratio, two original series were identified, $M_{2+x}An^{IV}_{2-x}An^{III}_x(C_2O_4)_5 \cdot nH_2O$(**1**) and $M_{1-x}[An^{III}_{1-x}An^{IV}_x(C_2O_4)_2 \cdot H_2O] \cdot nH_2O$(**2**) (M = single-charged cation), with hexagonal or tetragonal symmetry, respectively. Considering the An(IV)–Pu(III) pairs (An(IV) = Th, U, Np, Pu) and a Pu(III)/(An(IV) + Pu(III)) mole ratio close to 0.5, the structure of the precipitate is observed to evolve along the actinide series (Fig. 8). For An(IV) = Th or U, the precipitate is characterized by the hexagonal structure, whereas for An(IV) = Np or Pu, the solid compound crystallizes mainly in the tetragonal system.

At the same time, the influence of the An(III) nature (An(III) = Pu or Am) on the structure of the An(III)–U(IV) precipitates was investigated. For an An(III)/(U(IV) + An(III)) (An(III) = Am or Pu) mole ratio near 0.1, irrespective of the actinide(III) considered, the mixed An(III)–U(IV) oxalate adopts an hexagonal structure.

The sample preparation, which gives sometimes powder of low crystallinity, and the partial radiolysis induced by some isotopes were responsible for the low signal/background ratio which makes the refinement of the lattice parameters rather difficult. However, the unit cell parameters of An(IV)–An(III) mixed oxalate compounds were quite accurately refined by pattern matching using Fullprof [17] from X-ray powder of freshly synthesized powders. Only the lattice parameters of the $U(IV)_{90}$–$Pu(III)_{10}$ compound were not refined because of the poor crystallinity of the sample, although the comparison with the theoretical XRD pattern of the hexagonal structure indicates that the precipitate corresponds to a hexagonal mixed oxalate.

The decrease in the lattice parameters from Th(IV) to U(IV) for the hexagonal structure and from Np(IV) to Pu(IV) for the tetragonal structure is in agreement with the decrease of ionic radii along the actinide series [18] (Table 2).

The An(IV)–An(III) crystallographic mixed site is also responsible for the homogeneous distribution of actinides in the solids.

Table 2
Lattice parameters of An(IV)–An(III) mixed oxalate compounds

System	Structure	*a* (Å)	*c* (Å)
$Th0_{50}$(IV)–Pu_{50}(III)	Hexagonal	19.176(4)	12.735(5)
U_{50}(IV)–Pu_{50}(III)	Hexagonal	19.115(7)	12.664(5)
U_{90}(IV)–Am_{10}(III)	Hexagonal	19.203(8)	12.74(1)
Np_{50}(IV)–Pu_{50}(III)	Tetragonal	8.792(2)	8.018(3)
Pu_{50}(IV)–Pu_{50}(III)	Tetragonal	8.813(7)	7.97(1)

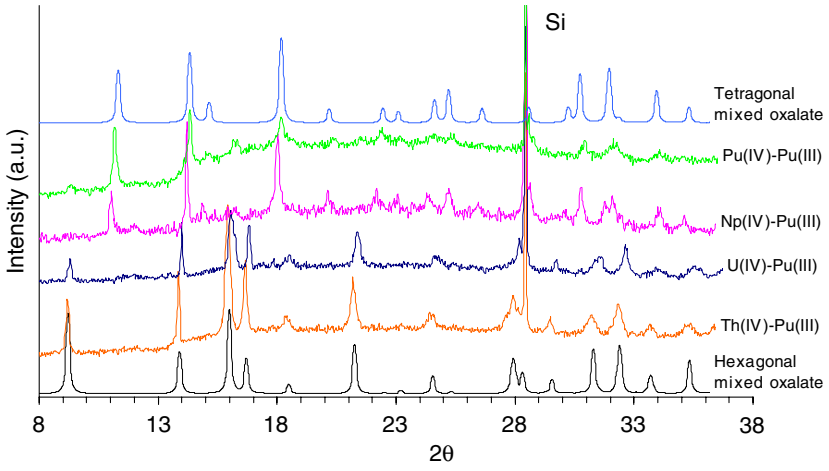

Fig. 8. XRD patterns of An(IV)–Pu(III) oxalate precipitates (An(IV) = Th, U, Np, Pu).

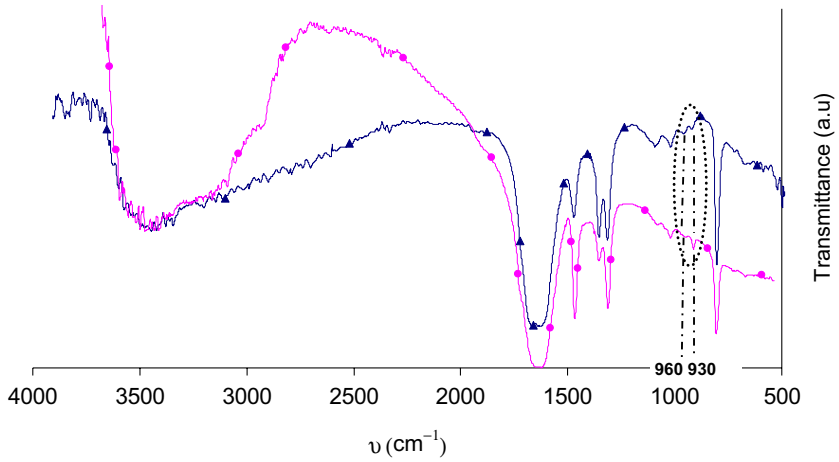

Fig. 9. Infrared spectra of An(IV)–An(III) oxalate precipitates: ● An(IV)–An(III) hexagonal mixed oxalate; ● An(IV)–An(III) tetragonal mixed oxalate.

3.2.3. Identification of monovalent cations

As in the previous case of mixed U(IV)–Ln(III) oxalates, infrared spectra of An(IV)–An(III) based precipitates are characteristic of oxalate compounds. Moreover, the presence of the two additional bands at 960 and 930 cm^{-1} assigned to the N–N stretching vibrations confirms the presence of hydrazinium cations within the structure (Fig. 9).

The results of hydrazinium cation titrations in mixed An(IV)–An(III) oxalates are in agreement with those obtained for U(IV)–Ln(III) compounds. In the hexagonal structure, the hydrazinium cation content is virtually constant and independent of the An(III)/(An(IV)+An(III)) mole ratio and the charge balance is ensured by H_3O^+ cations, whereas in the tetragonal compounds it appears that both cations, H_3O^+ and $N_2H_5^+$, take part in the electroneutrality of the structure.

Thermogravimetric experiments were carried out on the different mixed An(IV)–An(III) compounds and led to the determination of the water molecule content for each precipitate and consequently for each type of oxalate series (hexagonal or tetragonal).

4. Conclusion

These thorough investigations of the mixed U(IV)–Ln(III) oxalates synthesized by a co-precipitation method complete the structural data recently acquired on these compounds from single crystals obtained by the gel growth method. This work confirms the existence of two types of U(IV)–Ln(III) oxalate solid solutions (one adopting a hexagonal structure and the other a tetragonal one) and also illustrates the presence within the structure of an original mixed U(IV)–Ln(III) crystallographic site.

The extension of this structural study to actinide systems leads to the preparation and to the characterization of homeotype single-phase mixed An(IV)–An(III) oxalates. A range of mixed-valent uranium compounds [24–29] has previously been reported with different inorganic and/or organic ligands and different pairs of oxidation states (IV–V; IV–VI or V–VI). In most of these mixed-valence compounds, the environment of uranium atoms depends on the oxidation state. Hexavalent uranium, for instance, adopts a specific environment: it is always axially bonded to two oxygen atoms forming a uranyl unit with an O=U=O bond angle close to 180°. On the contrary, in the oxalates described in this paper, the tetravalent and trivalent actinides can adopt the same type of coordination sphere (nine or ten oxygen atoms from bidentate oxalate ligands and/or water molecules) and can then be disordered on the same crystallographic site. Original oxalate solid solutions formulated $(N_2H_5, H_3O)_{2+x}An^{IV}_{2-x}An^{III}_{x}(C_2O_4)_5 \cdot 4H_2O$ and $(N_2H_5, H_3O)_{1-x}[An^{III}_{1-x}An^{IV}_{x}(C_2O_4)_2 \cdot H_2O] \cdot 4H_2O$ are thus obtained. Finally, other types of An(IV)–An(III) mixtures and other $An^{III}/(An^{IV} + An^{III})$ mole ratios are now investigated to determine precisely the solid solution field of existence for each An(IV)–An(III) pair.

Acknowledgements

This research was financially supported by AREVA NC, France. We thank Jean Luc Emin, AREVA NC, France, for encouraging this work and for fruitful discussions.

References

[1] V. Matuha, S. Matuha, Actinides and Lanthanides oxalates, Atomic Energy Publ., Moscou, 2004.
[2] M.S. Grigor'ev, I.A. Charushnokova, N.N. Krot, A.I. Yanovskii, Yu.T. Struchkov, Radiochemistry 39 (1997) 420.
[3] I.L. Jenkins, F.H. Moore, J. Inorg. Nucl. Chem. 27 (1965) 77.
[4] W. Ollendorff, F. Weigel, Inorg. Nucl. Chem. Lett. 5 (1969) 263.
[5] A. Michaelides, S. Skoulika, A. Aubry, Mat. Res. Bull. 23 (1988) 579.
[6] K.K. Palkina, N.E. Kuz'mina, O.V. Koval'chukova, S.B. Strashnova, B.E. Zaitsev, Russ. J. Inorg. Chem. 46 (2001) 1348.
[7] M.N. Akhtar, A.J. Smith, Acta Crystallogr. B 31 (1975) 1361.
[8] M.C. Favas, D.L. Kepert, J.M. Patrick, A.H. White, J. Chem. Soc., Dalton Trans. 3 (1983) 571.
[9] I.A. Charushnokova, N.N. Krot, S.B. Katser, Radiochemistry 40 (1998) 558.

[10] B. Chapelet-Arab, S. Grandjean, G. Nowogrocki, F. Abraham, J. Solid State Chem. 178 (2005) 3046.
[11] B. Chapelet-Arab, S. Grandjean, G. Nowogrocki, F. Abraham, J. Solid State Chem. 178 (2005) 3055.
[12] B. Chapelet-Arab, L. Duvieubourg, F. Abraham, G. Nowogrocki, S. Grandjean, J. Solid State Chem. 179 (2006) 4003.
[13] Glenn T. Seaborg, Radiochim. Acta 61 (1993) 115.
[14] B. Chapelet-Arab, G. Nowogrocki, F. Abraham, S. Grandjean, J. Solid State Chem. 177 (2004) 4269.
[15] B. Chapelet-Arab, G. Nowogrocki, F. Abraham, S. Grandjean, Radiochimica Acta 93 (2005) 279.
[16] S. Grandjean, A. Bérès, J. Rousselle, C. Maillard, Brevet FR/04 51058, 2004.
[17] J. Rodrigez Carvajal, M.T. Fernandez Diaz, J.L. Martinez, J. Phys–Condens Mat. 3 (1991) 3215.
[18] R.D. Shannon, Acta Crystallogr. A32 (1976) 751.
[19] J. Hanuza, B. Jezowska-Trzebiatowska, C. Janczak, Acta Phys. Pol. A 45 (6) (1974) 885.
[20] S. Govindarajan, K.C. Patil, M.D. Poojary, H. Manohar, Inorg. Chim. Acta 120 (1986) 103.
[21] A. Braibanti, F. Dallavalle, M.A. Pellinghelli, E. Leporati, Inorg. Chem. 7 (1968) 1430.
[22] C.J. Mandleberg, K.E. Francis, R. Smith, J. Chem. Soc. (1961) 2464.
[23] J.A. Porter, Precipitation of neptunium oxalate and calcinations to neptunium oxide, Report No. DP-591, 1961.
[24] A.J. Zozulin, D.C. Moody, R.R. Ryan, Inorg. Chem. 21 (1982) 3083.
[25] F.A. Cotton, D.O. Marler, W. Schwotzer, Inorg. Chem. 23 (1984) 4211.
[26] S. Allen, S. Barlow, P. Shiv Halasyamani, J.F.W. Mosselmans, D. O'Hare, S.M. Walker, R.I. Walton, Inorg. Chem. 39 (2000) 3791.
[27] P.B. Duval, C.J. Burns, W.E. Buschmann, D.L. Clark, D.E. Morris, B.L. Scott, Inorg. Chem. 40 (2001) 5491.
[28] Chih-Min Wang, Chia-Hsien Liao, Hsiu-Mei Lin, Kwang-Hwa Lii, Inorg. Chem. 43 (2004) 8239.
[29] P. Bénard, D. Louër, N. Dacheux, V. Brandel, M. Genet, Chem. Mat. 6 (1994) 1049.